The Structure and Dynamics of the Corona – Heliosphere Connection

Spiro K. Antiochos · Jon A. Linker · Roberto Lionello · Zoran Mikić · Viacheslav Titov · Thomas H. Zurbuchen

Received: date / Accepted: date

Abstract Determining the source at the Sun of the slow solar wind is one of the major unsolved problems in solar and heliospheric physics. First, we review the existing theories for the slow wind and argue that they have difficulty accounting for both the observed composition of the wind and its large angular extent. A new theory in which the slow wind originates from the continuous opening and closing of narrow open field corridors, the S-Web model, is described. Support for the S-Web model is derived from MHD solutions for the quasi-steady corona and wind during the time of the August 1, 2008 eclipse. Additionally, we perform fully dynamic numerical simulations of the corona and heliosphere in order to test the S-Web model as well as the interchange model proposed by Fisk and co-workers. We discuss the implications of our simulations for the competing theories and for understanding the corona – heliosphere connection, in general.

Keywords Sun: corona · Sun: solar wind

1 Introduction

Since the pioneering theoretical work of Parker (1958, 1963) and the discovery observations of Neugebauer & Snyder (1962) it has been known that the Sun's atmosphere streams continuously outward in the form of a supersonic wind. This wind carries both plasma and magnetic field to the boundary of the solar system, the heliopause. At a basic level, the origins of the wind are straightforward. As argued by Parker, the difference in gas pressure between the Sun's hot, 1 MK, corona and the tenuous interstellar gas causes the coronal

S. K. Antiochos
NASA Goddard Space Flight Center, Code 674, Greenbelt, MD 20771, USA
Tel.: +1-301-286-8849
Fax: +1-301-286-1648
E-mail: spiro.antiochos@nasa.gov

J. A. Linker, R. Lionello, Z. Mikić, V. Titov
Predictive Science, Inc., 9990 Mesa Rim Rd., Ste. 170, San Diego, CA 92121, USA

T. H. Zurbuchen
Department of Atmospheric, Oceanic and Space Sciences, College of Engineering, University of Michigan, 2455 Hayward St, Ann Arbor, Michigan 48109

gas to expand outward. If the heating to the corona is constant, then the wind can adopt the steady state described by Parker's original theory.

Of course, on the real Sun there are many added complications to Parker's simple steady-state model. The first and foremost is the presence of the solar magnetic field. This naturally divides the corona into two physically distinct regions. In those regions where the field is strong, such as deep inside an active region, the field prevents the plasma from expanding; thereby resulting in an approximately static coronal plasma. These regions are referred to as "closed", because all field lines are connected to the photosphere at two ends. The closed flux is truly coronal in that it does not connect to the heliosphere, but appears instead as the well-known X-ray coronal loops (e.g., Orrall 1981). On the other hand, in those regions where the field is weak and the gas dominates, the gas pressure drags the field lines outward indefinitely. These regions are referred to as "open" in that the field lines have only one end connected to the photosphere. The outward mass and energy flow in open regions results in a decreased density there, so that they appear as "coronal holes" in X-ray images (e.g., Zirker 1977). Note that for a true steady state, the solar wind and the heliospheric magnetic flux originate solely from photospheric/coronal open-field regions.

In addition to introducing the complication of topology to the corona and heliosphere, the magnetic field also forces them to be fully time dependent. Since the distribution of flux at the photosphere is constantly changing due to flux emergence/cancellation and a broad range of photospheric flows, the distribution of open and closed flux must change, as well, implying that the solar wind is inherently dynamic. Consequently Parker's theory can be, at best, a quasi-steady approximation to the actual state of the corona and wind.

The dynamics introduced to the solar wind by the photospheric field evolution naturally breaks up into different regimes determined by the time required for establishing a steady wind. This is of order a few travel times to the Alfvén radius, ~ 20 $R_\odot$, which implies a time scale of ten hours or so. Since the photospheric evolution has a more-or-less constant speed of 1 km/s or less, the time scale translates directly to a size scale for the photospheric dynamics. Large-scale phenomena, such as the differential rotation or the emergence/dispersal of large active regions occurs over days, and so could be incorporated within the quasi-steady approximation. Small-scale phenomena, however, such as the magnetic carpet (Harvey 1985; Schrijver et al. 1997) or granular flows have time scales typically less than a few hours and, hence, can be considered as a constant source of fluctuations or noise to the quasi-steady state. Intermediate between these spatial scales is the typical size of supergranules, whose lifetimes are of order that required to establish a steady state. It is likely that their effect on the wind can be determined properly only by explicit time-dependent calculations.

In the heliosphere, the photospheric dynamics appear to structure the solar wind via the mediation of the magnetic field into two distinct forms, the so-called fast and slow winds. The fast wind has speeds generally in excess of 500 km/s, but that is not its distinguishing feature. This wind has 3 defining features: (a) its temporal variations, (b) spatial location, and (c) plasma composition.

(a) As shown clearly by the Ulysses measurements, the high-latitude fast wind exhibits near constant speed (McComas et al. 2008) and composition (Geiss et al. 1995; von Steiger et al. 1995; Zurbuchen 2007). Its observed variability consists primarily of Alfvénic fluctuations that may be due entirely to the expected dynamics induced by the small-scale photospheric evolution described above.

(b) The fast wind originates inside non-transient (lifetime $>$ 1 day) coronal holes, where the field has been open for a sufficient duration to establish a steady state.

(c) The fast wind has elemental abundances close to that of the photosphere (von Steiger et al. 1997, 2001; Zurbuchen et al. 1999, 2002). It does not exhibit the FIP bias of the closed-

field corona (Meyer 1985; Feldman & Widing 2003). Furthermore, its ionic composition is steady and implies a freeze-in temperature near the Sun around or below 1 MK (Zurbuchen 2007).

From these properties, we conclude that the fast wind is the true quasi-steady wind of the original Parker theory. The slow wind, on the other hand, is completely different. Its speeds are generally < 500 km/s, but again, this is not the distinguishing feature. The 3 defining features of this wind are markedly different than those above:

(a) The slow wind is intrinsically variable, both in speed and, especially, composition (Zurbuchen & von Steiger 2006; Zurbuchen 2007). The velocity structure consists of periods of fast flows intermingled with slow. This variation is not simply Alfvenic fluctuations superimposed on a quasi-steady state. Certainly the large compositional variability, both in elemental and ion-temperatures, cannot be due to turbulence in the flow, but reflects instead an intrinsic difference in the origins of the fast and slow wind.

(b) The slow wind is associated with the heliospheric current sheet (HCS), which is always embedded in slow wind, not fast (Burlaga et al. 2002). On the other hand, the slow wind is observed to extend in the heliosphere to angles far from the HCS, up to 30° or so.

(c) The slow wind has elemental composition (FIP bias) close to that of the closed field corona. Its ionic composition implies a freeze-in temperature near the Sun (~ 1.5 MK), considerably higher than that of the fast (Zurbuchen et al. 2002). Furthermore, the elemental and ionic compositions are highly variable, unlike the steady composition of the fast. A key point is that, as defined by the composition, the boundary between the fast and slow winds is narrow, of order a few degrees or so (Zurbuchen et al. 1999), which is small compared to the angular extent of either the slow or fast winds.

The results that the slow wind is associated with the HCS, which maps down to the Y-line at the top of the helmet streamer belt, and that the slow wind has the composition of the closed corona suggest that it somehow originates from near or inside the closed field region. The most obvious scenario is that it is due to the interaction between closed and open fields, which releases closed field plasma onto open field lines. This would naturally account for both its observed variability and composition. The problem, however, is that the slow wind does sometimes extend far from the HCS in latitude, which implies that its source at the Sun is inside the open field region, far from the open-closed field boundary. But in that case, it is difficult to understand why its composition should resemble that of closed field plasma. These apparently conflicting observations have long made the identification of the solar sources of the slow wind one of the major unsolved problems in Heliophysics. We describe below the basic theories that have been proposed for the slow wind sources, present some numerical tests of one of these theories (Linker et al. 2011), and describe a new theory for the slow wind, the S-Web model (Antiochos et al. 2011).

2 Theories for the Sources of the Slow Wind

There are essentially three different possibilities for the slow wind source: It originates in the open field region, just like the fast; it somehow originates from inside the closed field region; or it originates from the streamer tops, at the boundary between open and closed. We discuss each of them, in turn, below, but focus on the streamer top model and propose an extension of this theory, the S-Web model, that can reconcile the theory with observations.

2.1 The Expansion Factor Model

Perhaps, the simplest theory for the slow wind is that it originates from open field near the boundary between open and closed (Suess 1979; Kovalenko 1981; Withbroe 1988; Wang & Sheeley 1990; Cranmer & van Ballegooijen 2005; Cranmer et al. 2007). This scenario is highly appealing in that it implies a unified theory for the origins of the fast and slow winds. Both are due to a single mechanism: photospherically-driven MHD waves deposit heat and momentum to coronal plasma, resulting in a Parker-like solar wind outflow. The key idea underlying the model is that the speed of the wind is sensitive to the exact locations of the heat and momentum deposition in an open flux tube; in particular, heating low down below the critical point leads to a hotter, slower wind (Holzer & Leer 1980). The observed differences between the fast and slow winds, therefore, may arise solely from the geometrical difference between flux tubes near the coronal hole boundary versus those deep in the interior. Flux tubes near the boundary expand super-radially from the photosphere to a height of order a few solar radii; whereas those near the interior expand radially or even sub-radially. Even if the photospheric flux of waves into all flux tubes in a coronal hole is the same, the evolution of the waves in the corona, (the resulting turbulence and dissipation), will depend on the geometry of the flux tube. Cranmer and co-workers have argued that all the distinguishing features of the slow wind, including the variability and elemental composition can be explained by the effect of the flux tube geometry, the so-called expansion factor, on the wave evolution.

The challenge for the expansion factor theory is that the speed of the solar wind is sometimes observed to be slow, but the wind still has the variability, composition, and other features indicative of the fast wind. Zhao et al. (2009) have shown that the wind from small low-latitude coronal holes with large expansion factors is, indeed, slow, ~ 500 km/s; but this wind still has all the temporal and compositional characteristics of the fast wind. These observations are in direct conflict with any model proposing that the differences between the fast and slow wind result solely from differences in flux tube geometry. The Zhao et al. (2009) results demonstrate that a large expansion factor in an open flux tube does slow down the wind, as predicted, but it does not lead to the variability and composition observed in the slow wind. We conclude, therefore, that the expansion factor model, as presently described, is not consistent with the observations.

2.2 The Interchange Model

Another theory for the slow wind is the interchange model proposed by Fisk and co-workers (Fisk et al. 1998; Fisk 2003; Fisk & Zhao 2009), which in many ways is the diametric opposite of the expansion factor model. In the interchange model the slow wind is postulated to originate from the closed field region via continuous interchange reconnection between open field lines and the closed flux. Consequently, this model is intrinsically dynamic; there is no steady state solar wind, at least, for the slow component. Note also that there is no truly closed field region, because the open flux is postulated to diffuse throughout the apparently closed field regions outside coronal holes. The key idea underlying the model is that the evolution of the coronal open flux is dominated by the continuous small-scale dynamics of the photosphere, such as emergence/cancellation of magnetic carpet bipoles, which drive reconnection between open flux and closed. In addition to being fundamentally dynamic rather than steady, the interchange model also proposes a completely different magnetic topology than the expansion factor model. In the latter, the topology is smooth with well

separated open and closed field regions, but in the former the topology is essentially chaotic with open and closed flux mixing indiscriminately.

In terms of accounting for slow wind observations, the advantages of the interchange model are obvious. It naturally produces a continuously variable wind with closed field composition and located around the HCS, but with large extent. The primary challenge for the model is to verify that interchange reconnection induced by photospheric dynamics does, indeed, produce the required diffusion of open flux into closed field regions. Arguments have been presented by Antiochos et al. (2007) that basic Lorentz force balance considerations prohibit the mixing of open flux with closed. In fact, Antiochos et al argued that the open-closed topology remains smooth even during interchange reconnection and have proposed theorems that severely constrain the possible topologies of the Sun's open field regions. These authors, however, did not perform an actual dynamic calculation of the effect of interchange reconnection with magnetic carpet bipoles on open flux evolution. We present just such a calculation in the following section. As will be evident below, the results of this calculation do *not* support the underlying assumptions of the interchange model. Our results, however, do support key aspects of the interchange model in that dynamics and a statistical approach are likely to be essential for modeling the slow wind.

2.3 The Streamer-Top Model

The third theory for the source of the slow wind, the streamer-top model, is in some ways, a compromise between the expansion factor and interchange models. The basic idea is that the boundary between the open and closed flux, the edge of a streamer, is either unstable (Suess et al. 1996; Endeve et al. 2004; Rappazzo et al. 2005) or sensitive to perturbations and, consequently, undergoes continuous dynamics (Mikić et al. 1999). In response to photospheric changes or other disturbances, closed flux near the streamer boundary expands outward and becomes open and open flux reconnects at the HCS to become closed. Furthermore, interchange reconnection can occur at the streamer tops in response to photospheric changes (e.g., Wang et al. 2000). These processes will naturally release closed field plasma into the solar wind and produce a variable wind with the observed composition. Note that in this model the source of the slow wind is the boundary region between open and closed flux, similar to the expansion factor model, but the boundary in this case is fully dynamic and involves the continual interchange of open and closed flux. In this respect the model is similar to the interchange model, but the open-closed interchange in the streamer-top model occurs only near the streamer boundary. There is no diffusion of open flux deep inside the closed-field streamer.

There are a number of observations that provide compelling support for the streamer-top model. Movies of coronal evolution often show the upward expansion and eventual opening of closed loops (Hundhausen et al. 1984; Howard et al. 1985; Sheeley & Wang 2002). Conversely, coronagraph observations frequently show blobs streaming outward near the current sheet and reconnection events at the HCS (Sheeley 1997), as required for the streamer-top model. In the heliosphere the HCS is observed to be clearly dynamic with no evidence for a simple field reversal as would be the case for a quasi-steady wind. We conclude, therefore, that the boundary between the open and closed flux in the corona is, indeed, highly dynamic and, therefore, will be the source of a variable slow wind.

The problem, however, is that these dynamics are expected to be confined to a relatively narrow region about the streamer boundary, or equivalently, about the HCS. Assuming that the open-closed boundary is "blurred" by the photospheric dynamics over a scale of order a

supergranule radius, $\sim 30,000$ km, we derive an angular extent for this dynamic wind of no more than 5°. In fact, this width is what is observed for the streamer stalks emanating from the tops of streamers and for the so-called plasma sheet in the heliosphere (Winterhalter et al. 1994; Wang et al. 2007). But this angular width is far too small to explain the slow wind which has been observed to extend out to 30° from the HCS. Explaining the large angular extent of the slow wind is the fundamental challenge for the streamer-top model. Since the boundary between open and closed flux maps directly to the HCS, it seems unlikely that blurring this boundary by a small distance on the Sun would ever produce effects in the heliosphere far from the HCS. We describe below our theory, the S-Web model, that accomplishes exactly this unlikely result.

3 The S-Web Model

In previous work (Antiochos et al. 2007) we proposed the *uniqueness* conjecture, which states that any unipolar region on the photosphere can contain at most one coronal hole. However, low-latitude coronal holes that appear to be disconnected from their corresponding polar hole are frequently observed on the Sun (e.g., Kahler & Hudson 2002). We argued that in these cases, the low-latitude satellite hole is actually connected to the main polar hole by a narrow open field corridor whose width is below the spatial resolution of the observations. Note also that if the corridor is sufficiently narrow, it will be obscured by neighboring closed field regions with much higher brightness.

Let us consider how such a corridor would map into the heliosphere. For illustrative purposes, Figure 1 shows such a mapping in the extreme case where the polar hole and satellite holes have near equal flux. The inner hemisphere corresponds to the photosphere, with the dark yellow region representing the closed field and the light blue representing the two coronal holes connected by an open-field corridor. The light orange hemisphere corresponds to some surface in the heliosphere where the field is all open, say at 10 $R_\odot$. On this surface the radial flux is approximately uniformly distributed, as in the real heliosphere, and there is a single HCS, indicated by the black line running around the equator of the 10 $R_\odot$ surface. Note that this HCS maps down to the boundary of the single, (topologically connected), open field region on the photosphere. Four field lines with footpoints near the "end points" of the open field corridor are drawn, illustrating this mapping from the HCS to the open field boundary.

If the holes have roughly equal flux, their flux must divide the 10 $R_\odot$ surface into two near equal halves. In Fig. 1, the satellite hole maps to the near half and the polar to the far. Separating these halves is a thin arc, blue curve on the 10 $R_\odot$ surface, that maps to the open field corridor. Note that this arc divides the heliospheric surface and, hence, must extend to near 90° from the HCS. If the open-field corridor is very narrow, then the field-line mapping from the blue arc down to the solar surface is quasi-singular, so topologically, the arc is a so-called quasi-separatrix layer (Priest & Démoulin 1995; Démoulin et al. 1996; Titov et al. 2002). The HCS, on the other hand, is a true separatrix, because the field-line mapping is singular there.

Figure 1 illustrates a steady model, but to obtain the slow wind we need to add the temporal variability. Assume that due to the random photospheric evolution, the open-closed boundary at the photosphere becomes dynamically blurred by continuous field line opening and closing over some finite width, such as a supergranule scale. This narrow boundary region is now a source of slow wind. Due to the field line mapping, the HCS also acquires a finite angular width of order several degrees, and becomes a location for slow wind in the

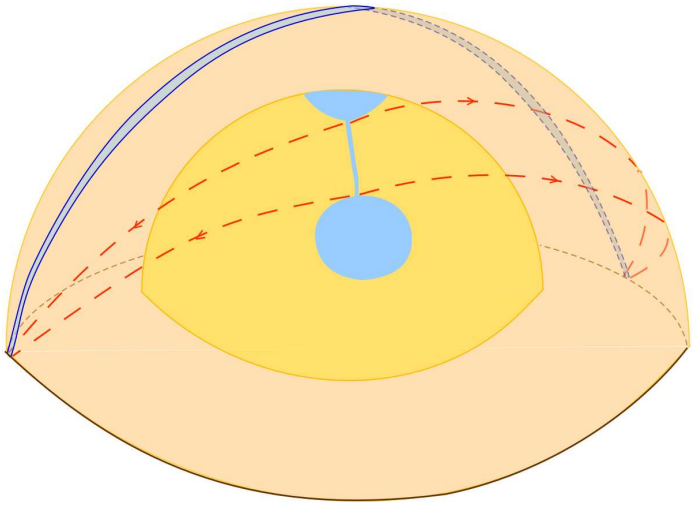

Fig. 1 Illustration of an open field corridor connecting two coronal holes (blue shading) at the photosphere (yellow inner surface), and its magnetic field line (red dashed) mapping to a heliospheric surface (pale orange).

heliosphere. But if the open field corridor is narrower than a supergranule scale, then *all* the flux in the corridor will be dynamically blurred by field line opening and closing and will be a source of slow wind. Since the corridor flux maps to the blue arc, this must also be a location of slow wind in the heliosphere. The key point is that the arc extends well above the HCS, so that in the case of Fig. 1, slow wind occurs up to 90° above the HCS, at the heliospheric pole!

Note that as long as it is narrower than a supergranule scale, the width of the open-field corridor is irrelevant to our arguments. Depending on the distribution of photospheric flux, Titov et al. (2011) have shown that the corridor can shrink down to the point it becomes the zero-width footprint of a separatrix dome. Regardless of whether a finite corridor or a singularity is present, this is a region where electric current concentrations would be expected to form when the footpoints of the fields are stressed by photospheric motions, and where the magnetic field is most susceptible to reconnection. Reconnection in turn allows plasma formed on closed field lines to access open fields and escape as part of the slow solar wind. Note that the instantaneous open-field boundary and resulting HCS are also of zero width, and yet, they produce a slow wind region of finite extent.

We conclude from the discussion above that open-field corridors and the topology of Fig. 1 may be able to reconcile the observed extent of the slow wind with the streamer top model. If this is the case, the main challenge to the model would be overcome. Of course, for a single corridor as in Fig. 1, the slow wind occurs only in a narrow arc of several degrees width, which is not sufficient to account for the observed slow wind, irrespective of where the arc lies. The important question, therefore is the number of such corridors and arcs for a true solar photospheric flux distribution.

To answer this question we calculated with very high numerical resolution, the steady state MHD solution for the corona and wind during a Carrington rotation centered about the August 1, 2008 eclipse (Rušin et al. 2010). Figure 2 shows the open and closed field distribution at the photosphere calculated from the model, along with the polarity inversion

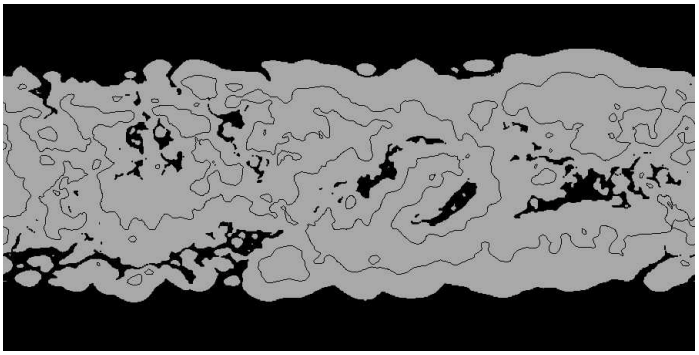

Fig. 2 Distribution of open magnetic flux (black) and closed (grey) at the photosphere for a Carrington rotation centered about Aug. 1, 2008. Also shown is the polarity inversion line on a surface slightly above the photosphere, *(adapted from Antiochos et al 2011)*.

line slightly above the photosphere (for clarity). It is evident that during this time period there were numerous satellite holes extending from the main polar holes.

Figure 3 shows the distribution of the squashing factor, Q, on the heliospheric surface at 10 $R_\odot$. The squashing factor is a robust topological measure that allows for straightforward identification of quasi-separatrix layers and separatrices (Titov et al. 2002, 2008). We note that surrounding and connected to the HCS (thick dark red line) is a dense web of high Q layers, the S-Web.

The S-Web of Fig. 3 is exactly what is needed to account for the slow wind observations. At some locations it extends up to 30° from the HCS, which explains the observations of slow wind at high latitudes. The HCS is not always symmetrically located inside the S-Web but can lie near one edge and, in fact, the HCS is often observed in the heliosphere to occur close to one of the slow wind boundaries rather than symmetrically between them (Burlaga et al. 2002). Although the Q layers are densely spaced, they are not space filling, so we expect that the wind in the S-Web region will actually consist of a mixture of slow and fast, as observed. Note also, that the S-Web has a clearly defined boundary separating it from the polar flux regions, which can account for the observed sharp transition between slow and fast wind (Zurbuchen et al. 1999).

We conclude that, at least, for the time period of August 2008, the open-field corridors at the photosphere and the S-Web in the heliosphere have all the necessary topological structure to produce the observed slow wind. Of course, the underlying assumption is that when the photospheric dynamics are added to the model, magnetic field will open and close as required, and a sufficient amount of closed field plasma will be released into the heliosphere. We describe below a simulation which represents our first step towards adding dynamics to the S-web model.

4 Coronal and Heliospheric Dynamics

It is not yet possible to perform a fully time-dependent calculation that adequately resolves dynamics such as reconnection occurring on the smallest scales shown in Fig. 2. Even relaxing this configuration to a steady state strained our computational resources! Adding the magnetic carpet and its complex evolution to the calculation is well beyond present capabilities. Therefore, we consider instead a simplified scenario in which we begin with an

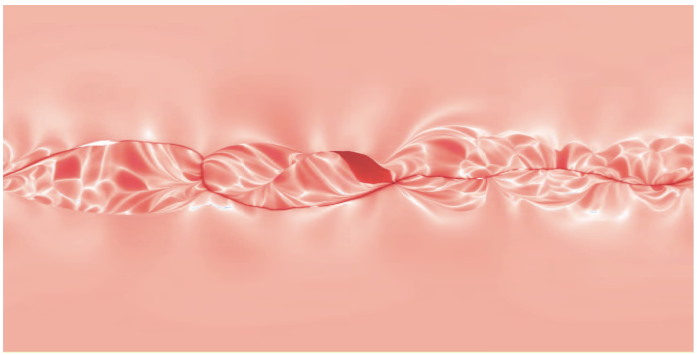

Fig. 3 Distribution of Q-factor on a heliospheric surface at 10 $R_\odot$ for the coronal hole system of Fig. 2. The HCS appears as the dark red line and the contours of high Q as white, *(adapted from Antiochos et al. 2011)*

observed photospheric flux distribution, but less structured than in Fig. 2, and two "magnetic carpet" bipoles. Rather than attempting to emerge and submerge the flux, which is also difficult computationally, we only convect the bipoles with a simple photospheric motion.

Although this simulation does not allow for a full test of the S-web model, it does test whether open-field corridors form and coronal holes stay connected in a fully dynamic evolution. It also determines whether the field opens and closes in response to photospheric dynamics, as required. Furthermore it provides a severe test of the interchange model. According to this model, interchange reconnection leads to the diffusion of open flux into the closed. We expect that there will be substantial interchange reconnection as the bipoles move; hence, if the interchange model is correct, the open and closed field regions will become highly mixed.

4.1 The Numerical Model

We use spherical coordinates and advance in time the following set of viscous and resistive MHD equations (in cgs units):

$$\nabla \times \mathbf{B} = \frac{4\pi}{c}\mathbf{J}, \tag{1}$$

$$\nabla \times \mathbf{E} = -\frac{1}{c}\frac{\partial \mathbf{B}}{\partial t}, \tag{2}$$

$$\mathbf{E} + \frac{\mathbf{v}\times\mathbf{B}}{c} = \eta \mathbf{J}, \tag{3}$$

$$\frac{\partial \rho}{\partial t} + \nabla\cdot(\rho\mathbf{v}) = 0, \tag{4}$$

$$\frac{1}{\gamma - 1}\left(\frac{\partial T}{\partial t} + \mathbf{v}\cdot\nabla T\right) = -T\nabla\cdot\mathbf{v}, \tag{5}$$

$$\rho\left(\frac{\partial \mathbf{v}}{\partial t} + \mathbf{v}\cdot\nabla\mathbf{v}\right) = \frac{1}{c}\mathbf{J}\times\mathbf{B} - \nabla p + \rho\mathbf{g} + \nabla\cdot(\nu\rho\nabla\mathbf{v}), \tag{6}$$

where $\mathbf{B}$ is the magnetic field, $\mathbf{J}$ is the electric current density, and $\mathbf{E}$ is the electric field. In practice the vector potential $\mathbf{A}$ is advanced, with $\mathbf{B} = \nabla\times\mathbf{A}$. The variables ρ, $\mathbf{v}$, p, and T are the plasma mass density, velocity, pressure, and temperature, $\mathbf{g} = -g_0\hat{\mathbf{r}}/r^2$ is the

gravitational acceleration, η the resistivity, ν is the kinematic viscosity, and $\gamma = 1.05$ is the polytropic index. The polytropic approximation is adequate for this study, since we are interested primarily in the magnetic field evolution rather than the detailed plasma energetics as in Lionello et al. (2009). The boundary conditions are discussed by Linker & Mikić (1997) and Linker et al. (1999). At the inner radial boundary, a fixed temperature of 1.8×10^6 K and an electron density of 10^8 cm^{-3} are prescribed. The component of the velocity along the magnetic field is not specified but calculated from the characteristic equations. At the outer radial boundary the flow is supersonic and super-Alfvénic, and variables are computed with the aid of the characteristic equations.

The grid is nonuniform in $r \times \theta \times \phi$ of $151 \times 191 \times 291$ points, with $\Delta r \approx 2.6 \times 10^{-3}\ R_\odot = 1.8$ Mm at the lower radial boundary and $\Delta r \approx 0.75\ R_\odot$ at $20\ R_\odot$. The latitudinal mesh varies between $\Delta\theta \approx 3.7^\circ$ at the poles and $\Delta\theta \approx 0.5^\circ$ near the equator. The azimuthal (longitudinal) mesh varies between $\Delta\phi \approx 0.5^\circ$ in the primary region of study to $\Delta\phi \approx 3.0^\circ$ further away. The simulation domain extends out to $20R_\odot$. The Alfvén travel time at the base of the corona ($\tau_A = R_\odot/V_A$) for $|\mathbf{B}| = 2.205$ G and $n_0 = 10^8$ cm^{-3}, which are typical reference values, is 24 minutes (Alfvén speed $V_A = 480$ km/s). A uniform resistivity is chosen such that the Lundquist number τ_R/τ_A is 1×10^5, where τ_R is the resistive diffusion time. A uniform viscosity ν is also used, corresponding to a viscous diffusion time τ_ν such that $\tau_\nu/\tau_A = 500$. Again, this value is chosen to dissipate unresolved scales without substantially affecting the global solution. During the phases of the simulation where reconnection occurs, the length scales are considerably smaller than $1R_S$ and the numerical dissipation exceeds the specified η, so the Lundquist number is consequently smaller in the regions where these dynamics occur.

On the solar surface, the bottom boundary, we prescribe for the magnetic flux distribution a smoothed NSO Kitt Peak map for Carrington Rotation (CR) 1913 (August 22 – September 18, 1996). The resulting coronal hole pattern shows a long southward extension of the northern coronal hole, the so-called Elephant's Trunk (Gibson et al. 1999) that was visible during this time period, Figure 4. To study the effects of photospheric dynamics on this system, we add two small bipoles in the area around the Elephant's Trunk, top panel in Fig. 4. The northern bipole produces a small closed field region inside the coronal hole, while the southern bipole results in a small satellite coronal hole connected to the rest of the Elephant Trunk by an open field corridor, Fig. 4. Note that although it has considerable fine-scale structure, the open field topology in Fig. 4 is topologically smooth and well-connected.

We then drive this system with a surface flow that is uniform in longitude and directed from west to east, $v_{\phi 0} \approx -1$ km/s between $30.5^\circ \leq$ Lat. $\leq 36.0^\circ$, and between $7.8^\circ \leq$ Lat. $\leq 15.3^\circ$. This flow causes the bipoles to move through the open and closed field regions and, in particular, across the open-closed boundaries. We stop the flow after 70 hours and allow the system to relax further for 14 hours.

4.2 Results and Conclusions

Fig. 4 shows the open and closed flux at the photosphere at four times during the evolution. The dynamics of this evolution are dominated by two basic processes: flux opening and closing at the HCS and interchange reconnection at the moving bipoles. Each of them is discussed, in turn, below.

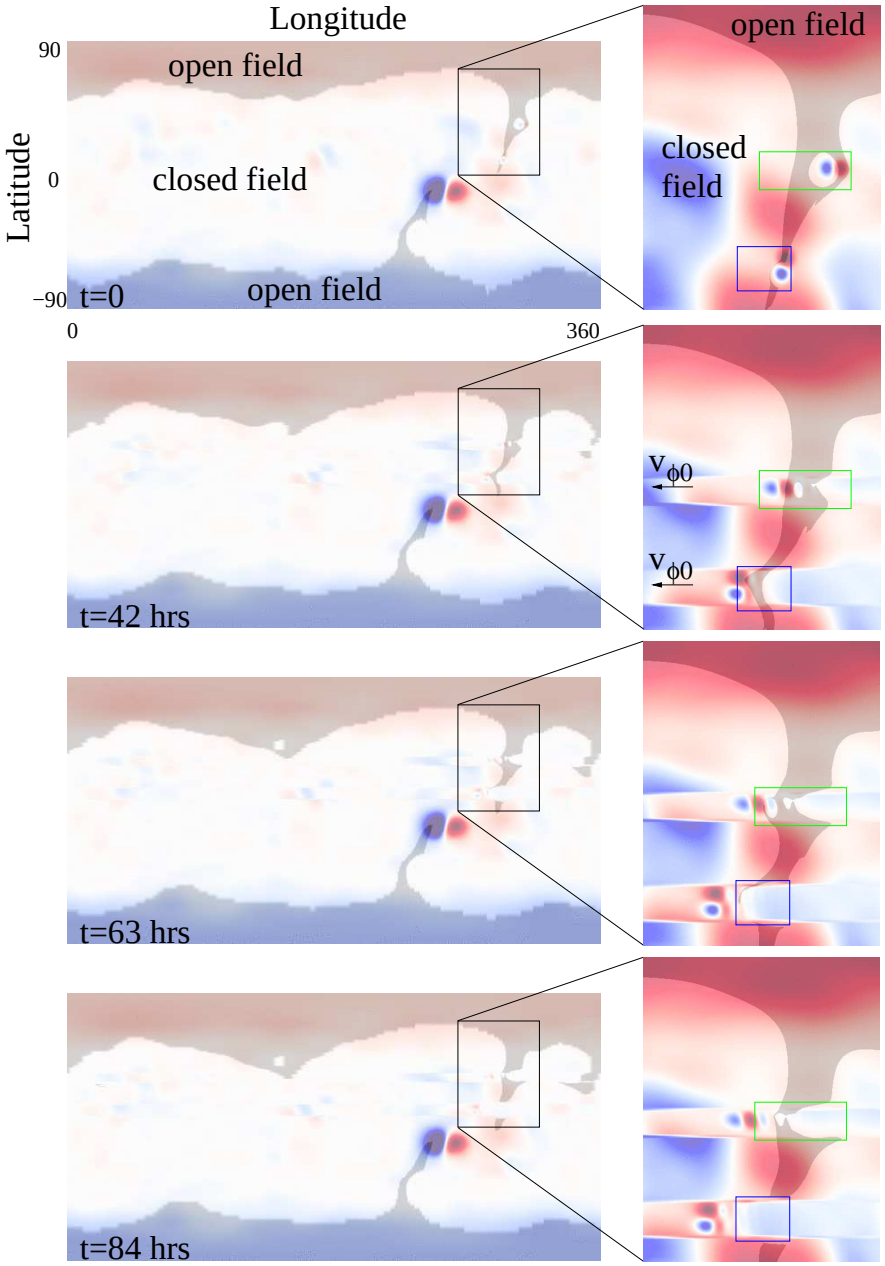

Fig. 4 Evolution of the open and closed flux at the photosphere for the case of two small bipoles driven by a uniform surface flow from west to east. The top panel shows the initial field. Open flux regions are indicated by gray shading and superimposed over color contours (red and blue) of the normal photospheric flux, *(adapted from Linker et al. 2011)*

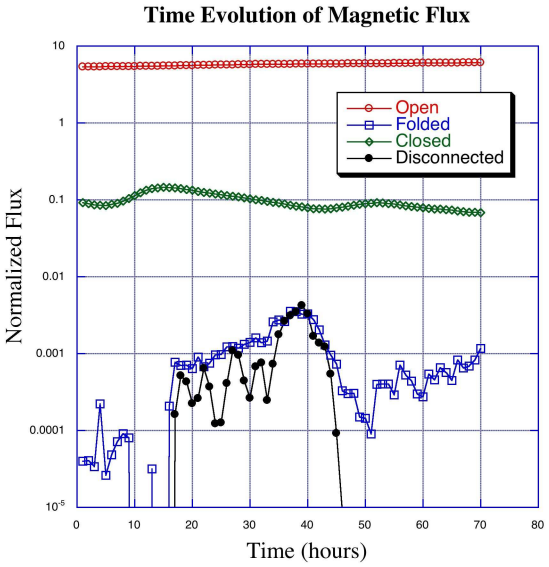

Fig. 5 Evolution of the open, closed, disconnected, and folded (interchange reconnected) flux intersecting the 10 $R_\odot$ surface during the course of the simulation.

4.2.1 Flux Opening and Closing

We find that as a result of the magnetic stress (electric currents) added to the coronal field by the photospheric motions, the field tends to expand outward in the vicinity of the bipoles. This outward expansion upsets the force balance between gas and field at the streamer tops, so that some of the field there "opens", i.e., expands outward past the simulation outer boundary. As the bipoles continue to move, however, the extra stress may be relieved locally and the streamers relax back down via reconnection of open flux, which creates closed and disconnected flux. The disconnected flux is then convected outward by the wind and exits the system, while the closed flux returns the streamer to its pre-stressed state.

Note that for a fully dynamic system, such as the real heliosphere, the concept of open and closed field lines becomes somewhat imprecise. For our simulation, we define a field line that at any instant has both its footpoints on the photosphere and lies fully within our domain, out to 20 $R_\odot$, as closed. Any field line that has one footpoint on the outer boundary is open and any field line with both footpoints on the outer boundary is disconnected.

Figure 5 shows the evolution of the various flux systems that intersect the r = 10$R_\odot$ surface during the course of the simulation. Since the Figure shows only the flux through the 10 $R_\odot$ surface, most of the closed flux in the simulation domain is not included, as well as any disconnected flux that lies between the 10 $R_\odot$ and 20 $R_\odot$ surfaces. We find, however, that the disconnection reconnection occurs near the bottom of the HCS, < 5 $R_\odot$; consequently, Fig. 5 measures all the disconnected flux during its initial evolution. Of course, all the disconnected flux eventually leaves the domain.

Fig. 5 verifies the basic premise of the streamer-top and S-web models. In response to photospheric stressing, magnetic flux opens and closes at the HCS. Although we do not track it explicitly, there is clearly release of closed field plasma into the wind. For the localized boundary motions of our simulations, the flux opening/closing is small; we note from Fig. 5 that the open flux increases only slightly during the simulation and the disconnected flux is always 3 orders of magnitude or more smaller than the open. If we were to impose random motions throughout the photosphere, as in the Sun, the flux opening and closing would be much more pronounced. The key point, however, is that there is definitely opening and closing at the HCS, in agreement with the S-web model, but in direct conflict with the basic premise of the interchange model (Fisk et al. 1998; Fisk 2003).

An important conclusion from our results is that closed and disconnected flux should be continuously present in the heliosphere near the HCS. In fact the HCS is well known to be a region of continuous dynamics; for example, the field is rarely observed to vanish there as would be expected for a true steady state. On the other hand, closed and disconnected field lines should exhibit distinct electron heat-flux signatures in the heliosphere (e.g., Gosling 1990; McComas et al. 1991). These signatures are frequently observed in ICMEs, which clearly do involve substantial flux opening and closing, but they are rarely seen outside CMEs (Gosling 1990; Pagel et al. 2005), suggesting that the slow wind flux is not opening and closing. Reconciling this apparent disagreement with the heliospheric electron heat flux measurements, which may require re-interpretation of the electron data (Crooker & Pagel 2008), remains one of the major challenges for all solar wind models.

4.2.2 Interchange Reconnection

The other major form of dynamics found in our simulation is that of interchange reconnection between the flux of the small bipoles and the surrounding field. The magnetic topology of each bipole is simply that of the well-known embedded bipole with its fan separatrix surface, pair of spine lines, and coronal null point (e.g., Antiochos 1990; Antiochos et al. 2007). The photospheric motions stress the separatrix and null, creating current sheets there, which leads to reconnection between the closed field associated with the parasitic polarity of the bipole and the external flux (see Figure 6). If this flux is open, then the reconnection is of the interchange type; if it is closed, the reconnection merely exchanges closed flux (Edmondson et al. 2009; Linker et al. 2011).

Since interchange reconnection, like all reconnection, occurs at a strong current concentration, it is likely to produce an open field line with a sharp bend or "fold", Fig. 6). Sharp field line bends cannot occur as a result of the slow photospheric driving, because bends in the field tend to propagate away Alfvénically before they reach nonlinear amplitudes. Consequently, we can obtain an estimate of the amount of interchange reconnection by measuring the amount of open flux intersecting the 10 $R_\odot$ surface that is folded. Fig. 5 shows the result. Note that almost all of this "folded" flux is located near the bipoles, so it is likely to be due to interchange reconnection at the bipoles. Furthermore, the flux in Fig. 5 yields only a lower limit on the amount of interchange reconnection.

As evident from the sequence of images in Fig. 4, the effect of the interchange reconnection is to allow the bipole flux to transfer smoothly across coronal hole boundaries. Consider, for example, the northern bipole. The closed parasitic polarity is initially completely inside the Elephant Trunk coronal hole. Due to the photospheric stressing, however, this closed flux region interchange reconnects with the surrounding open, and transfers toward the coronal hole boundary on the east. It is important to emphasize that the "motion" of the bipole flux is not that of a simple translation due to the boundary flows. The photospheric flows move

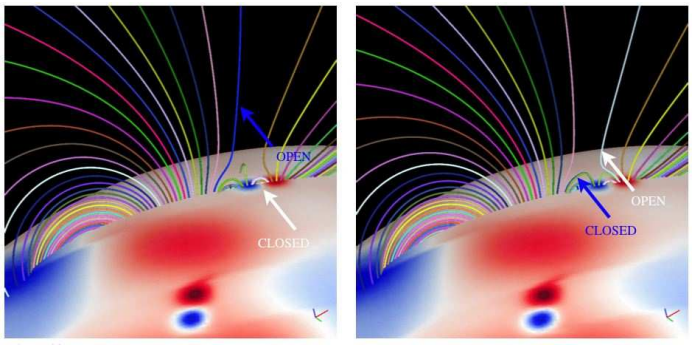

Fig. 6 Interchange reconnection results from advection of a bipole. B_r is contoured on the surface, with red for positive polarity and blue for negative polarity. Field lines are traced from fixed positions on the surface, in the same simulation as Fig. 5. In the left-hand frame, an open field in blue and a closed field line in white are identified. As bipole flux advects past, (right-hand frame) the previously closed location transitions to open and the previously open location closes down. Note that as the white field line, for example, undergoes the transition from closed (left) to open (right) it develops a very sharp bend or "fold", which can be used as a signature for interchange reconnection.

all the flux; therefore, if the evolution were purely ideal, the coronal hole boundary would move eastward along with the bipole and the bipole would never change its topology. The bipole flux can move across the coronal hole boundary only by reconnection (or diffusion).

The key result of Fig. 4 is that in spite of the extreme distortions caused by the sharp gradients in the boundary flows and especially by interchange reconnection, the open field region remains topologically connected (Linker et al. 2011). We do not find the type of open-closed field mixing required for the interchange model (Fisk 2003). It is evident that open flux is not transported into the closed field region. Hence, we conclude that slow wind cannot originate from the closed field region. Of course, our simulation has only two bipoles, whereas, the magnetic carpet consists of many, but we see no reason to expect that this fundamental conclusion will change by merely superimposing more bipoles.

We expect, therefore, that even in the true corona, which includes the complexity of the magnetic carpet, closed field regions are rigorously closed and the assumptions of the interchange model do not apply there. Note, however, that in the open field regions the effect of the motions of many bipoles, the magnetic carpet, would be to induce continuous and ubiquitous interchange reconnection. Consequently, the basic ideas of the interchange model (Fisk 2003), may well be applicable, but *only inside coronal holes*.

Another important result is that the basic idea of the *uniqueness* conjecture is confirmed in that there is only one open field region throughout the simulation. On the other hand, the connections between the various sections of the Elephant Trunk obviously develop a complex and sometimes singular geometry. In particular, by the end of the simulation, $t = 84$ hours, the far southern tip of the Trunk and the rest of the coronal hole are not connected by an open field corridor of finite flux, but are merely *linked* by a separatrix curve with vanishing width, as described in detail by Titov et al. (2011). For the purposes of the S-web model, the width of the corridor or link is unimportant as long as it connects up to the open field and produces a quasi-separatrix arc there that extends far from the HCS. More important is that there be a large number of coronal hole corridors and links. The photospheric flows we impose do produce these structures, but these flows are not a good representation of actual photospheric motions.

Perhaps, the most important conclusion of this paper is the importance of dynamics. Given the extreme fine structure inferred from the observations, Fig. 2, and seen in the calculations, Fig. 4, it seems inescapable that understanding the origins of the slow solar wind will require fully dynamic models of the corona - heliosphere connection. The calculations presented here represent a first step toward a fully dynamic S-Web model.

Acknowledgements This work originated from numerous discussions in a LWS Focus Team on open flux in the heliosphere. The work was funded, in part, by the NASA HTP, GI, SR&T, and TR&T Programs, by CISM (an NSF Science and Technology Center), and by Strategic Capabilities (jointly funded by NASA, NSF, and AFOSR). Computational resources were provided by the NSF supported Texas Advanced Computing Center (TACC) in Austin and the NASA Advanced Supercomputing Division (NAS) at Ames Research Center.

References

Antiochos, S. K. 1990, Mem. Soc. Astron. Italiana, 61, 369
Antiochos, S. K., DeVore, C. R., Karpen, J. T., & Mikić, Z. 2007, Astrophys. J., 671, 936
Antiochos, S. K., Mikić, Z., Titov, V. S., Lionello, R., & Linker, J. A. 2011, Astrophys. J., in press
Burlaga, L. F., Ness, N. F., Wang, Y.-M., & Sheeley, N. R. 2002, J. Geophys. Res., 107(A11), 1410, doi:10.1029/2001JA009217
Cranmer, S. R. & van Ballegooijen, A. A. 2005, Astrophys. J. Supp., 156, 265
Cranmer, S. R., van Ballegooijen, A. A., & Edgar, R. J. 2007, Astrophys. J. Supp., 171, 520
Crooker, N. U. & Pagel, C. 2008, J. Geophys. Res., 113, A02106, doi:10.1029/2007JA012421
Démoulin, P., Henoux, J. C., Priest, E. R., & Mandrini, C. H. 1996, Astron. Astrophys., 308, 643
Edmondson, J. K., Lynch, B. J., Antiochos, S. K., De Vore, C. R., & Zurbuchen, T. H. 2009, Astrophys. J., 707, 1427
Endeve, E., Holzer, T. E., &Leer, E. 2004, Astrophys. J., 603, 307
Feldman, U. & Widing, K. G. 2003, Space Science Rev., 107, 665
Fisk, L. A., Schwadron, N. A., & Zurbuchen, T. H. 1998, Space Science Rev., 86, 51
Fisk, L. A. 2003, J. Geophys. Res., 108, 1157
Fisk, L. A. & Zhao, L. 2009, in Universal Heliospheric Processes, Proc. IAU Symp. 257, 109
Geiss, J., Gloeckler, G, & von Steiger, R. 1995, Space Science Rev., 72, 49
Gibson, S. E., Biesecker, D., Guhathakurta, M., Hoeksema, J. T., Lazarus, A. J., Linker, J., Mikic, Z., Pisanko, Y., Riley, P., Steinberg, J., Strachan, L., Szabo, A., Thompson, B. J., & Zhao, X. P. 1999, Astrophys. J., 520, 871
Gosling, J. T. 1990, in Physics of Magnetic Flux Ropes, ed. C. T. Russell., E. R. Priest, & L. C. Lee, (AGU Geophys. Monograph 58), 373
Harvey, K. L. 1985, Aust. J. Phys., 38, 875
Hoeksema, J. T. 1991, Adv. Space Res., 11, 15
Holzer, T. E. & Leer E. 1980, J. Geophys. Res.85, 4665
Howard, R. A., Sheeley, N. R., Jr., Michels, D. J., & Koomen, M. J. 1985, J. Geophys. Res., 90, 8173
Hundhausen, A. J., Sawyer, C. B., House, L., Illing, R. M. E., & Wagner, W. J. 1984, J. Geophys. Res., 89, 2639
Kahler, S. W. & Hudson, H. S. 2002, Astrophys. J., 574, 467
Kovalenko, V. A. 1981, Solar Phys., 73, 383
Linker, J. A., & Mikić, Z. 1997, in Geophys. Monogr. 99: Coronal Mass Ejections, AGU, Washington, ed. N. Crooker, J. Joselyn, & J. Feynman, 269278
Linker, J. A., Mikić, Z., Biesecker, D. A., Forsyth, R. J., Gibson, S. E., Lazarus, A. J., Lecinski, A., Riley, P., Szabo, A., & Thompson, B. J. 1999, J. Geophys. Res., 104, 9809
Linker, J. A., Lionello, R., Mikić, Z., Titov, V. S., & Antiochos, S. K. 2011, Astrophys. J., in press
Lionello, R., Linker, J. A., & Mikić, Z. 2009, Astrophys. J., 690, 902
McComas, D. J., Phillips, J. L., Hundhausen, A. J., & Burkepile, J. T. 1991, Geophys. Res. Lett., 18, 73
McComas, D. J., et al. 2008, Geophys. Res. Lett., 35, L18103
Meyer, J.-P. 1985, Astrophys. J. Supp., 57, 173
Mikić, Z., Linker, J. A., Schnack, D. D., Lionello, R., & Tarditi, A. 1999, Phys. Plasmas, 6, 2217
Neugebauer, M. & Snyder, C. W. 1962, Science, 138, 1095
Orrall, F. Q. 1981, Solar active regions: A monograph from SKYLAB Solar Workshop III, Boulder, CO, Colorado Associated University Press

Pagel, C., Crooker, C. U., & Larson, D. E. 2005, Geophys. Res. Lett., 32, L14105, doi:10.1029/2005GL023043
Parker, E. N. 1958, Astrophys. J., 128, 664
Parker, E. N. 1963, Interplanetary Dynamic Processes, (New York: Interscience Publishers)
Priest, E. R., & Démoulin, P. 1995, J. Geophys. Res., 100, 23443
Rappazzo, A. F.,Velli, M., Einaudi, G., & Dahlburg, R. B. 2005, Astrophys. J., 633, 474
Rušin, V., Druckmüller, M., Aniol, P., Minarovjech, M., Saniga, M., Mikić, Z., Linker, J. A., Lionello, R., Riley, P., & Titov, V. S. 2010, Astron. Astrophys., 513, A45
Schrijver, C. J. et al. 1997, Nature, 48, 424
Sheeley, N. R., Jr., 1997, 1997, Astrophys. J., 484, 472
Sheeley, N. R., Jr. & Wang, Y.-M. 2002, Astrophys. J., 579, 874
von Steiger, R., Schweingruber, R. F., Wimmer, R., Geiss, J., & Gloeckler, G. 1995, Adv. Space Res.y, 15(7), 3
von Steiger, R., Geiss, J., & Gloeckler, G. 1997, in Cosmic Winds and the Heliosphere, eds. J. R. Jokipii, C. P. Sonett, & M. S. Giampapa (Tucson: Arizona U Press), p. 581.
von Steiger, R., Zurbuchen, T. H., Geiss, J., Gloeckler, G., Fisk, L. A., & Schwadron, N. A. 2001, Space Science Rev., 97, 123
Suess, S.T. 1979, Space Science Rev.23, 159
Suess, S.T., Wang, A-H. & Wu, S. T. 1996, J. Geophys. Res.101, 19957
Titov, V. S., Démoulin, P., & Hornig, G. 1999, in Magnetic Fields and Solar Processes, ESA SP-448, 715T
Titov, V. S., Hornig, G., & Démoulin, P. 2002, J. Geophys. Res., 107, 1164
Titov, V. S., Mikić, Z., Linker, J. A., & Lionello, R. 2008, Astrophys. J., 675, 1614
Titov, V. S., Mikić, Z., Linker, J. A., Lionello, R., & Antiochos, S. K. 2011, Astrophys. J., in press
Wang, Y.-M., & Sheeley, N. R. 1990, Astrophys. J., 355, 726
Wang, Y.-M., Sheeley, N. R., Socker, D. G., Howard, R. A., & Rich, N. B. 2000, J. Geophys. Res., 105(A11), 25133
Wang, Y.-M., Sheeley, N. R., Jr., & Rich, N. B. 2007, Astrophys. J., 658, 1340
Winterhalter, D., Smith, E. J., Burton, M. E., Murphy, N., & McComas, D. J. 1994, J. Geophys. Res., 99(A4), 6667
Withbroe, G. L. 1988, Astrophys. J., 325, 442
Zhao, L., Zurbuchen, T. H., & Fisk, L. A. 2009, Geophys. Res. Lett., 36, CiteID L14104, doi:10.1029/2009GL039181
Zirker, J. B. 1977, Coronal Holes and High Speed Wind Streams, (Boulder: Colorado Assoc. University Press)
Zurbuchen, T. H., Hefti, S., Fisk, L. A., Gloeckler, G., & von Steiger, R. 1999, Space Science Rev., 87, 353
Zurbuchen, T. H., Fisk, L. A., Gloeckler, G., & von Steiger, R. 2002, Geophys. Res. Lett., 29, 66, doi: 10.1029/2001GL013946
Zurbuchen, T. H., & von Steiger, R. 2006, in SOHO 17: 10 years of SOHO and Beyond, ed. H. Lacoste & B. Fleck, (Noordwijk, ESA), SP-617, p. 7.1
Zurbuchen, T. H. 2007, Ann. Rev. Astron. Astrophys., 45, 297